The Retina of *Spalax ehrenbergi*: Novel Histologic Features Supportive of a Modified Photosensory Role

Rafael Cernuda-Cernuda,[1] *Willem J. DeGrip,*[2] *Howard M. Cooper,*[3] *Eviatar Nevo,*[4] *and José M. García-Fernández*[1]

Purpose. The retina of the blind mole rat *Spalax ehrenbergi* was compared with other vertebrate photosensitive organs in an attempt to correlate its histologic organization with a presumptive nonvisual photoreceptor role.

Methods. The eyes of eight adult animals were analyzed by light and electron microscopy, using conventional staining and immunolabeling with antibodies against phototransduction proteins and calretinin.

Results. Rods accounted for most of the photoreceptor cells in the *Spalax* retina, although their morphology is dissimilar to that of sighted mammals, in that they contained only rudimentary outer segments. The latter showed strong rod-opsin and transducin immunoreactions. The phagosomes in the retinal pigmentary epithelium were also rod-opsin positive. Synapses were evident at the photoreceptor cells pedicles. Occasionally, several synaptic active sites were present, suggesting cone cell origin; however, cone-opsin was not immunodetected in the study samples. Synaptic ribbon fields, sometimes distant to the active sites, resembled those found in the vertebrate pineal. The other retinal layers were somewhat less organized than in sighted mammals. Some cells were displaced and the calretinin-positive inner plexiform layer had no sublayers. Calretinin immunolabeling was found in horizontal, amacrine, and ganglion cells. Folding of the retina produced rosette-like images similar to those reported before in the retina of nocturnal mammals and in the avian pineal gland.

Conclusions. These data suggest that the retina of the mole rat has undergone evolutionary restructuring to a photoreceptive pineal-like organization. This supports the thesis that the photoreceptor cells of this unique organ have been reprogrammed during the subterranean adaptation of *Spalax*, from their original visual function to mediating photoperiodic regulation. (*Invest Ophthalmol Vis Sci.* 2002;43:2374–2383)

Evidence has been presented recently that the visual photoreceptors are not required for the effect of light on the circadian axis. Naturally occurring mutant and transgenic mice that have no rods and cones, but maintain an apparently normal inner retina, are capable of photoregulating circadian locomotor activity rhythms and pineal melatonin levels in a manner indistinguishable from wild-type control animals.[1–4] It is also known that cognitively and clinically blind humans may retain the ability for acute suppression of serum melatonin in response to light exposure.[5] Thus, some class of nonrod, noncone photoreceptor, probably located in the inner layers of the retina, is suggested to function as the mammalian circadian photoreceptor.

Of all mammals, the subterranean mole rat, *Spalax ehrenbergi*, is reported to possess the most rudimentary eyes. Although ocular development initially proceeds normally, soon the lens starts to degenerate and the eye remains subcutaneous. Only the retina appears to mature unperturbed.[6] In addition to the eyes, the optic nerve regresses.[7] Retinal projections to visual nuclei, although present, have been observed to be severely atrophied.[8] Nonetheless, preservation of a functional photoreceptor role of the retina is indicated by the persistence of a significant projection from the retina, innervating a well-developed suprachiasmatic nucleus (SCN). In fact, light exposure during the dark phase induces c-fos expression in the ventral region of the SCN, where retinal afferents terminate.[9] In agreement with this, entrainment of circadian locomotor and thermoregulatory rhythms by ambient light has also been demonstrated. The removal of the eyes leads to a failure to adapt to these photoperiodic stimuli.[10] This suggests that this animal has retained a mechanism for photoperiodic perception and circadian regulation. The genes *Clock* and *MOP3*, involved in circadian rhythmicity, were recently cloned and sequenced and their expression studied in *Spalax*.[11] Given the degenerate lens and the location of the eyes, completely buried beneath the skin and embedded within a hypertrophied harderian gland, it is highly unlikely that the eye can still process visual image information. Indeed, morphologic structures involved in image analysis and visually guided behavior are reduced in size by more than 90% and show a poorly differentiated cytoarchitecture.[7] Behavioral and electrophysiological studies have confirmed that *Spalax* has no image-forming ability and is visually blind.[12] This species thus constitutes an extremely interesting naturally blind animal model for the study of the input of circadian information into the central nervous system.

Meanwhile, extensive data have become available on the functional properties of *Spalax* visual opsins[13,14] and of the *Spalax* visual system,[7,12] but only scattered data are available on the morphologic aspects of this very interesting retina at an ultrastructural level.[6]

Herein, we present a comprehensive morphologic study of the *Spalax* retina, which fully supports a functional photoreceptor role. Furthermore, we compare this unique organ to other vertebrate photosensitive organs in an attempt to correlate its structural organization with its presumed physiological role.

Methods

Eight adult individuals, four males and four females, of *Spalax judaei* (with diploid chromosome number 2n = 60), of the subpopulation of Anza (Israel), were used for this study. *S. judaei* is one of the four

From the [1]Department of Morphology and Cellular Biology, University of Oviedo, Spain; the [2]Department of Biochemistry, NCMLS, University of Nijmegen, The Netherlands; the [3]National Institute of Health and Medical Research, Lyon, France; and the [4]Institute of Evolution, University of Haifa, Israel.

Supported by European Union Grant Biomed-2, PL96-2327 (WJDeG, HMC, JMG-F).

Submitted for publication December 10, 2001; revised March 14, 2002; accepted March 22, 2002.

Commercial relationships policy: N.

The publication costs of this article were defrayed in part by page charge payment. This article must therefore be marked "*advertisement*" in accordance with 18 U.S.C. §1734 solely to indicate this fact.

Corresponding author: Rafael Cernuda-Cernuda, Departamento de Morfología y Biología Celular (8ª planta), Facultad de Medicina, Universidad de Oviedo, 33071 Oviedo, Spain; rcernuda@correo.uniovi.es.

chromosomal species in Israel belonging to the *Spalax ehrenbergi* superspecies.[15] The animals were maintained alive for a short period under low-intensity light conditions in a 12-hour light–darkness cycle and fed carrots and water ad libitum. All were anesthetized with diethyl ether and perfused transcardially for 20 minutes, during the light period. The eyes were dissected and fixed by immersion. The type of fixative used for perfusion and subsequent immersion, as well as the fixation time, were dependent on the planned type of analysis, as discussed later.

All experiments were approved by the local committees for Animal Care and Use and conformed to the ARVO Statement for the Use of Animals in Ophthalmic and Vision Research.

The immunohistochemical (IHC) study of the samples was performed by both light microscopy (LM) and electron microscopy (EM). The following antisera were used (polyclonal except where indicated): (1) rho 4D2, a monoclonal antibody against purified rod outer segments of rat, which is monospecific for rod photoreceptors in mammalian species[16]; (2) CERN-886 and CERN-JS858, which were raised against bovine rod rhodopsin; (3) CERN-906, which was elicited against chicken red and green cone opsins; (4) CERN-9412, which labels the α-subunit of the bovine rod transducin.

The CERN antibodies were developed in rabbits at the Department of Biochemistry, NCMLS, University of Nijmegen (The Netherlands), and their specificity was demonstrated previously.[1,14,17–19]

Besides the listed antisera against phototransductory proteins, anticalretinin (SWant Antibodies, Bellinzona, Switzerland), raised against the calcium-binding protein calretinin was used. This antibody has been shown to be a good marker of amacrine cells and their processes, which reach into different areas in the inner plexiform layer (IPL) in the mouse.[20] It was used to visualize the distribution of this cell type and also to probe the organization of the IPL.

For the IHC study at the LM level, samples fixed in Bouin fixative or 4% paraformaldehyde for 48 hours at 4°C, were dehydrated in ethanol and embedded in paraffin. Four-micrometer-thick sections were obtained with an ultramicrotome (Ultracut; Reichert-Jung, Vienna, Austria), using glass knives, and collected in double-gelatinized glass slides. After deparaffination in xylene, sections were rehydrated gradually in ethanol and once in distilled water, and single labeling with the antisera (dilution 1:2000–1:3000) was performed, using a peroxidase-conjugated avidin-biotin complex staining kit (Vectastain; Vector Laboratories, Burlingame, CA) as a detection system. Labeled sections were dehydrated in ethanol, cleared in xylene, mounted in a hydrophobic medium, and examined at the LM level.

For the IHC study at the EM level, samples were fixed in a phosphate-buffered (0.1 M, pH 7.3) 4% paraformaldehyde+0.25% glutaraldehyde solution for 2 hours at room temperature, washed in distilled water, dehydrated in ethanol and embedded in acrylic resin (LRWhite; London Resin Co., Basingstoke, UK). Ultrathin (approximately 80-nm thick) middle cross sections of the eyes, were obtained with the ultramicrotome, by using a diamond knife, and mounted on nickel grids. The primary antibodies (final concentration, 1:1000) were CERN-886, CERN-JS858, and CERN-9412. Afterward, grids were processed according to a standard immunogold protocol,[21] using 10 nm gold particles bound to rabbit IgG as a secondary antibody, counterstained with uranyl acetate, examined, and photographed in a transmission electron microscope (TEM; model EM 109; Carl Zeiss, Oberkochen, Germany).

To label possible apoptotic nuclei, the in situ terminal transferase-mediated nick end labeling (TUNEL) technique (commercial kit; Roche Molecular Biochemicals, Mannheim, Germany) was used on 4-μm-thick paraffin sections.[22] In addition, the semithin and ultrathin sections were screened for the presence of apoptotic nuclei according to standard morphologic criteria.[23]

For morphologic studies at the LM and EM level, samples were fixed in a phosphate-buffered (0.1 M, pH 7.3) 3% paraformaldehyde+2.5% glutaraldehyde solution for 2 hours at room temperature, postfixed in 1% OsO_4 at 4°C for 2 hours, washed in distilled water, dehydrated in acetone, and embedded in an Araldite-based resin (Durcupan; Fluka, Buchs, Switzerland). Semithin (1-μm thick) and ultrathin (approximately 80-nm thick) sections were obtained in the ultramicrotome, using glass and diamond knives, respectively. Semithin sections were stained with toluidine blue solution and examined at the LM level. Ultrathin sections, mounted on copper grids and stained with lead citrate and uranyl acetate, were viewed and photographed in the TEM.

LM images were recorded with a digital camera mounted on a microscope (camera model DMC; Polaroid, Cambridge, MA; microscope model Eclipse E400; Nikon, Tokyo, Japan). TEM photographic negative films were digitized using a scanner (SprintScan 35 Plus; Polaroid). The figures selected were arranged in plates using image management software (Corel Draw ver. 8.0; Corel Corp., Ottawa, Ontario, Canada).

Results

The eyes of *S. ehrenbergi* were approximately 1 mm in diameter and were located deeply under the skin, partially surrounded by the harderian gland (Fig. 1). A pigmented cap corresponding to the iris was detectable in the front side (Fig. 2, asterisk), but the surrounding areas were poorly pigmented. Most of the eyes studied did not have the pupil, which seemed to be collapsed by the accumulated pigment.

A middle cross-section of the eye shows that the crystalline lens was reduced to an amorphous vascularized structure. The anterior chamber was missing or indistinguishable. The choroid layer, which was reduced in width, had no pigment. The retinal pigment epithelium (RPE) also was poorly pigmented (Figs. 3, 4). Nevertheless, the main layers, typical of the stratified mammalian retina were all present. Usually, the stratification of the retinal layers was very clear (Fig. 3), but occasionally the outer nuclear layer (ONL) and outer plexiform layer (OPL) appeared to be less organized (Fig. 4).

The layer between the outer limiting membrane (OLM) and the RPE, which we will refer to as the outer neural retina (ONR; Fig. 4), showed normal inner segments (IS) of the photoreceptor cells (PCs); however, at the LM level, the outer segments (OS) seemed to be reduced or missing.

In the semithin sections, several different types of nuclei, corresponding to different cell types that will be described later, were distinguished in the inner nuclear layer (INL; Fig. 4). Furthermore, a cell type with metachromatic cytoplasm was present throughout the entire retina, but was more abundant in the INL and OPL (Fig. 4). Sometimes these cells were also observed in the ONL.

At the EM level, the ONR showed signs of abnormal photoreceptor morphology (Fig. 5). The OLM was clearly distinguishable, the PCs had well preserved IS (Figs. 5, 6, and 7), but did not contain normal OS. Only whorls of membranes that resembled rudimentary OS were visible (Fig. 5). Occasionally, these rudimentary elements were noted to be connected to the cilia (Fig 6, c). Rod-opsin–like immunoreactivity (IR) was abundant in these rudimentary OS, but was also detected in the plasma membrane of the cilia and the IS (Fig. 6). Whorls of membranes, hereafter referred to as myeloid bodies, also were localized within the IS and within other parts of the photoreceptor cells, but these bodies did not show any rod IR. Cisterns of rough endoplasmic reticulum (rER) and many mitochondria were found in the IS as well (Fig. 7). These rER cisterns did not show any rod-opsin IR, either (Fig 8), whereas such IR was observed throughout the plasma membrane of the PCs (Fig. 9). The antibody CERN-9412 (anti-rod transducin α-subunit) at the LM level labeled only a narrow area under the RPE, corresponding to the photoreceptor outer segments (not shown). In the EM images, CERN-9412 reactivity was detected in the whorls of membranes of the rudimentary OS (Fig. 10), but labeling of the

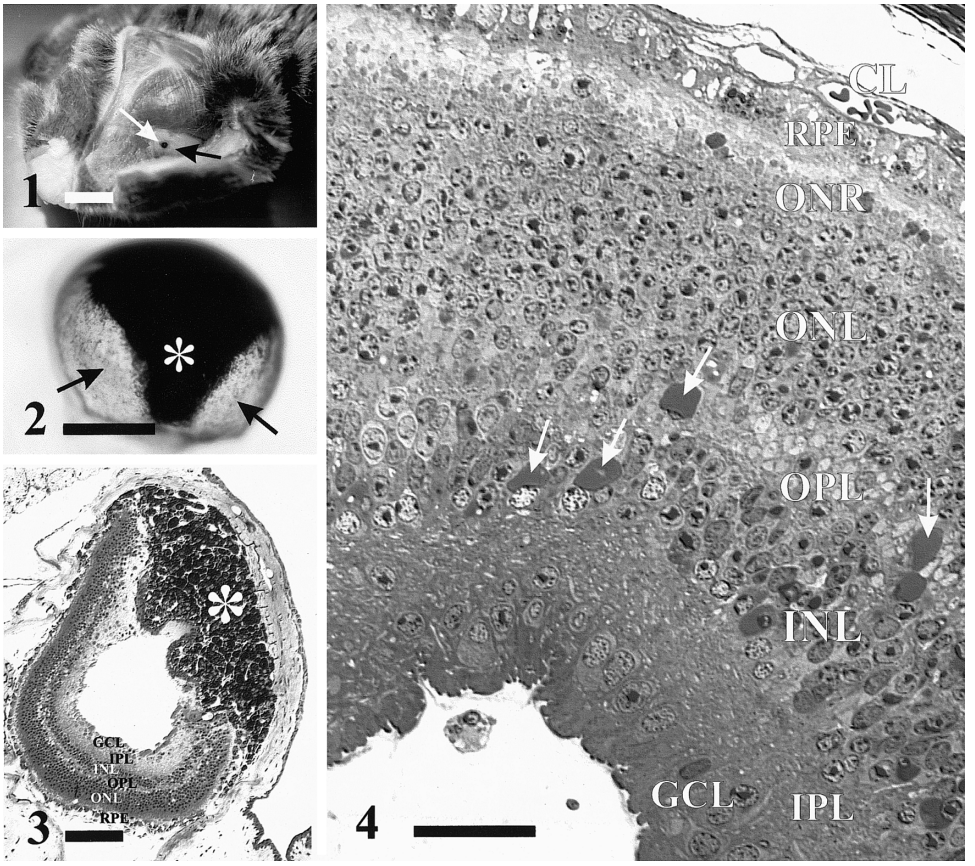

Figure 1. Once the animal had been perfused transcardially with the fixative solution, dissection of the head skin brought the eyes into view. The micrograph shows one of the eyes (*white arrow*), surrounded by the harderian gland (*black arrow*). Bar, 1 cm.

Figure 2. Accumulated pigment (✻) was noted in a frontal view of the eye. However, pigment was absent in the areas surrounding the frontal cap (*arrows*). Bar, 0.4 mm.

Figure 3. A semithin cross section of the eye shows a layered retina. (✻) Frontal pigment. Bar, 100 μm.

Figure 4. At a higher magnification, this semithin section permitted observation of the different layers of the retina in more detail. Below the RPE, a narrow ONR without a layer of normal outer segments was seen. The remaining layers of the retina are indicated. *Arrows:* metachromatic cells found in different locations, mainly in the INL and in the OPL. Bar, 40 μm.

plasma membrane of the PC was not observed. The RPE contained phagosomes that also showed rod-opsin labeling (Fig. 11).

Occasionally, folds or invaginations were observed in the outer layers of the retina. Rosette-like structures, corresponding to cross sections of these folds, could be seen in deep regions, such as the INL (Fig. 12). Cilia, some of which were cross-sectioned, clearly displayed the normal 9(2)+0 microtubular pattern (Fig. 12a).

The round nuclei of the photoreceptor cells exhibited prominent nucleoli and abundant heterochromatin (Fig. 13), and the cytoplasm showed numerous cisterns of rER and supranuclear Golgi apparatus (Fig. 13). No rod-opsin–like labeling was found associated with the rER or the Golgi cisterns. Free ribosomes, polyribosomes, and sometimes diverse ribosome-composed structures were also detected in these cells (Fig. 14).

Although synaptic structures, such as groups of ribbons and spherules surrounded by vesicles of electrolucent content were occasionally observed in places as distant as the IS of the PCs (Fig. 15), most of these structures were seen in subnuclear locations, either separated or close to the synaptic active sites (Fig. 16). Myeloid bodies, such as were described in the IS, also were common features of the subnuclear cytoplasm (Fig. 14).

The OPL, which mainly represents photoreceptor endings and cellular processes of the INL, was rather well developed. Numerous synaptic contacts were observed, and photoreceptor cell pedicles occasionally showed a complex organization, with several synaptic active sites (Fig. 17). Rod-opsin–like immunolabeling extended to the plasma membrane of most of the pedicles (Fig. 18), although with lower density than in the OS. Indeed, with all three antibodies used against rod-opsin, labeling over the entire ONL was found in LM sections, confirming the EM observations.

Some cells showing wide cytoplasmic areas without organellae, corresponding to the metachromatic cells observed in semithin sections, were seen dispersed through both the ONL and INL (Fig. 19) and occasionally in the ganglion cell layer (GCL). Their nuclei, which were round and heterochromatic, resembled those of PCs. Furthermore, synaptic structures (Figs. 19, 19a) and single cilia (Fig. 20) were also present in these cells.

Rod-opsin labeling of displaced photoreceptor cells was clearly observed at the LM level (Fig. 21). In fact, labeling of the plasma membrane was seen at the EM level in these cells with both the CERN-858 and the CERN-886 antibodies (Fig. 22).

The anti-calretinin antibody labeled several cellular somata present in both the inner and the outer margins of the INL,

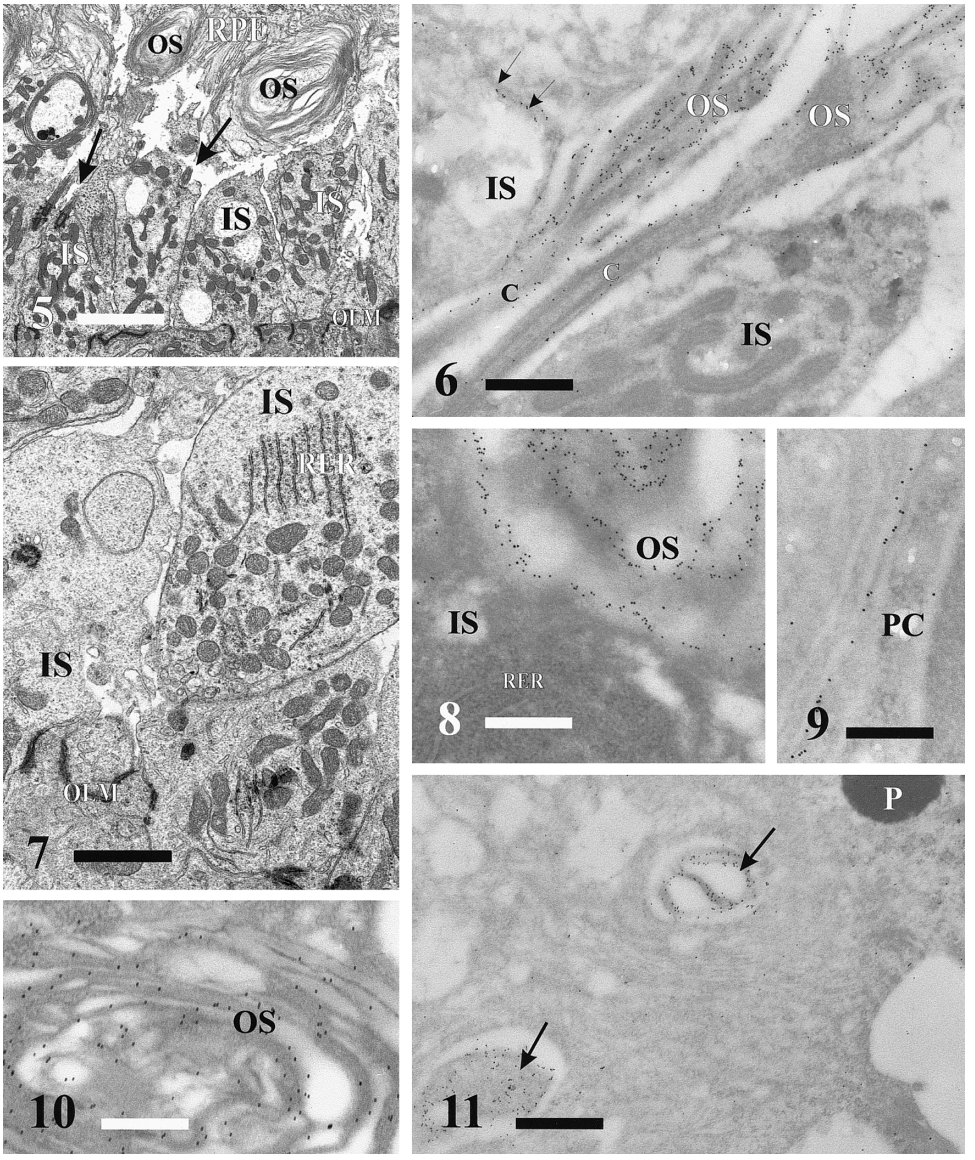

Figure 5. Examples of whorls of membranes observed in the outer neural retina, which correspond to rudimentary outer segments (OS). Cilia (*arrows*) inserted in the IS were easily detected. Bar, 2 μm.

Figure 6. The CERN-886 anti-rhodopsin antibody labeled the rudimentary OS, as well as the membrane surrounding cilia (C) and IS of the photoreceptor cells. The OS clearly derive from cilia. *Arrows*: gold particles in the plasma membrane of an IS. Bar, 2 μm.

Figure 7. Some IS exhibited cisterns of rER and an abundance of mitochondria. Bar, 2 μm.

Figure 8. The rER cisterns in the IS did not show any rod-opsin labeling. Note the very clear labeling in the OS (CERN-886). Bar, 3 μm.

Figure 9. Rod-opsin IR was also detected in the plasma membrane of the PC somata. This image shows labeling with the CERN-858 antibody. Bar, 4 μm.

Figure 10. The CERN-9412 anti-transducin α-subunit antibody labeled only the OS. Bar, 5 μm.

Figure 11. The phagosomes (*arrows*) in the RPE were also rod-opsin immunopositive, indicating active OS turnover. P, pigment granule. Bar, 2 μm.

corresponding to a subpopulation of horizontal and amacrine cells, respectively, and also in the GCL (Fig. 23). The OPL and IPL were labeled as well, but no sublayers were seen in the IPL (Fig. 23), such as those observed in other rodents.

In none of the sections examined was evidence found of the presence of apoptotic cells, as indicated by the absence of any nuclei showing either the typical apoptotic morphology[23] or positive labeling with the TUNEL assay (not shown).

At the EM level, the INL presented differentiated cell types (Fig. 24). Müller cells displayed round or oval dense nuclei; remarkably, some of these nuclei were displaced toward the ONL. We attempted to classify the remainder of the nuclei mainly by their position in the INL. Nuclei located in the horizontal cell sublayer, close to the OPL, were round and less electrodense than those of Müller cells (Fig. 24). The amacrine cell sublayer was occupied by cells with large, round electrolu-

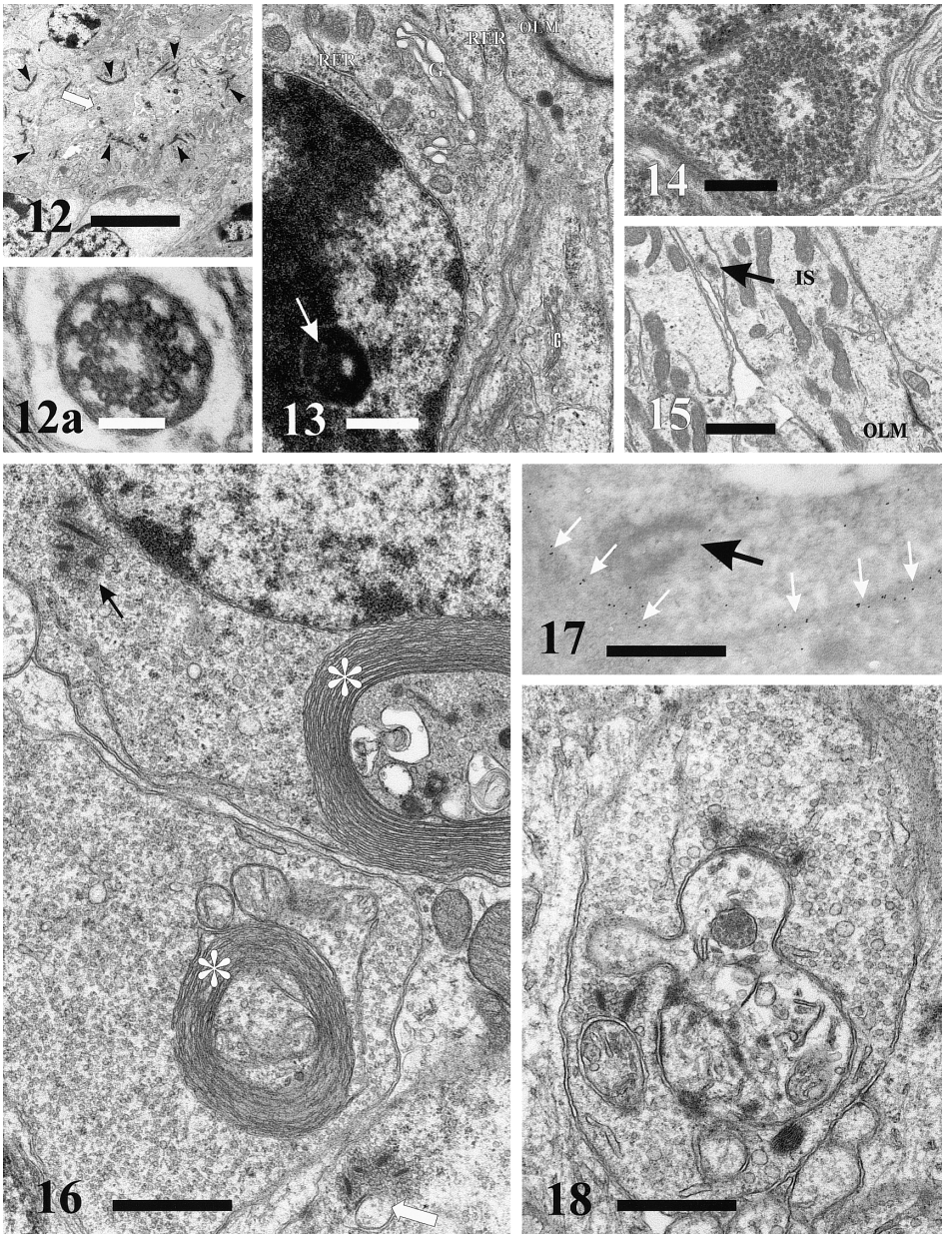

FIGURE 12. Rosette-like structures were found in the INL. *Black arrowheads*: densifications of the OLM. *White arrow*: a cross-sectioned cilium, shown at higher magnification in Figure 12a. Bar, 10 μm.

FIGURE 12A. Cross-sectioned cilia in these rosette-like structures display the normal 9(2)+0 pattern of microtubules. Bar, 0.1 μm.

FIGURE 13. The nuclei of PCs have abundant heterochromatin and a prominent nucleolus (*white arrow*). rER, mitochondria, and well-developed Golgi apparatus (G) were seen in the supranuclear region of these cells. Bar, 1 μm.

FIGURE 14. Occasionally, peculiar ribosomal formations were observed in photoreceptor cells. Bar, 0.25 μm.

FIGURE 15. Some synaptic ribbons were seen in locations very distant to the photoreceptor pedicle. The image shows two of them (*arrow*) found in a photoreceptor cell IS. Bar, 1 μm.

FIGURE 16. PCs often contained myeloid bodies (✻). In addition, this image shows a synaptic ribbon field that was apparently not associated with any active site (*black arrow*) and another one located close to a likely bipolar dendritic process (*white arrow*). Bar, 1 μm.

FIGURE 17. Rod-opsin IR reached the PC pedicles. The micrograph shows CERN-858 immunolabeling. *Black arrow*: two synaptic ribbons; *white arrowheads*: opsin-IR in the plasma membrane. Bar, 0.5 μm.

FIGURE 18. Occasionally, complex photoreceptor pedicles were observed. This micrograph shows one of them with four ribbons at their active synaptic sites. Bar, 0.5 μm.

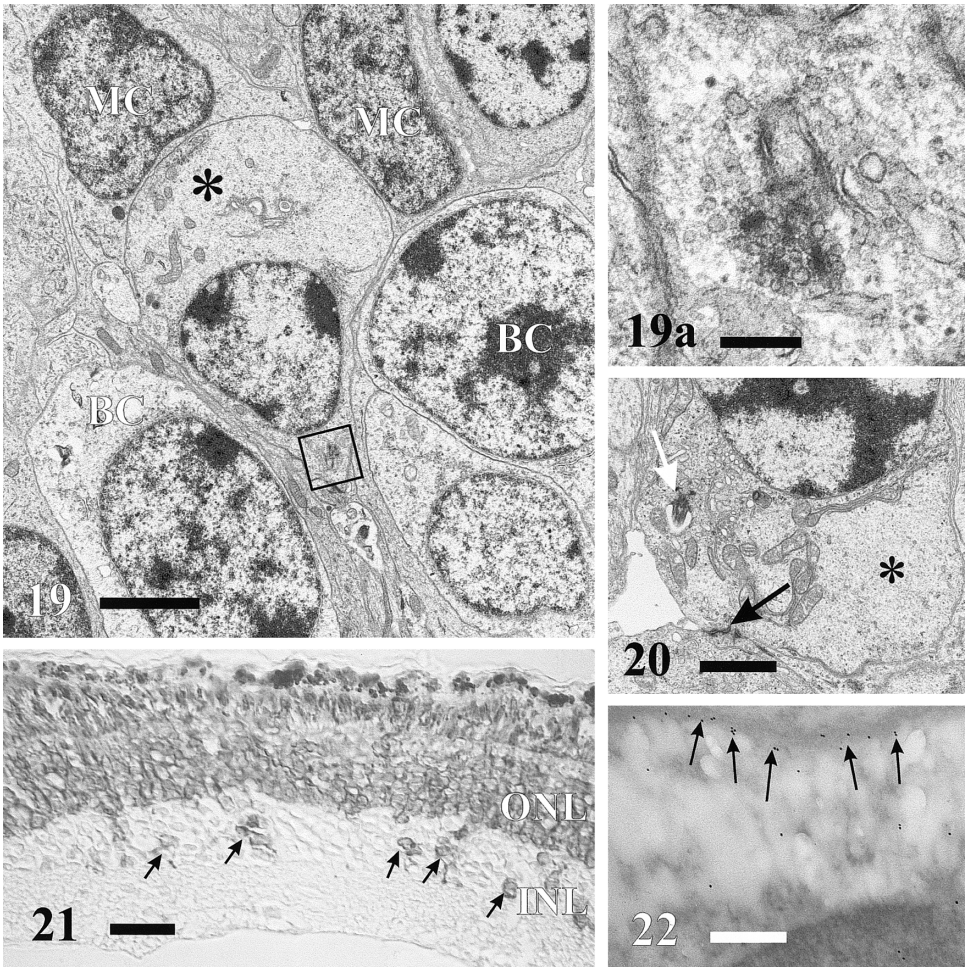

FIGURE 19. Some photoreceptor cells with wide cytoplasmic areas lacking organellae (✻) were observed in diverse locations. The image shows one of them located in the INL. *Box*: a synaptic ribbon field, which is magnified in Figure 19a. MC, Müller cell; BC, bipolar cell. Bar, 2 μm.

FIGURE 19A. Detail of the synaptic ribbon field indicated in Figure 19. Bar, 0.25 μm.

FIGURE 20. A cell similar to that shown in Figures 19 and 19a with a cilium (*white arrow*) and adherent junctions (*black arrow*) corresponding to the OLM. (✻) cytoplasmic area without organellae. Bar, 1 μm.

FIGURE 21. Anti-rod-opsin labeling extended into the ONL and was also found in some of displaced PCs in the INL (*arrows*). Bar, 25 μm.

FIGURE 22. Ultrastructural analysis showed that the rod-opsin labeling in these displaced cells was located in the plasma membrane (*arrows*). Bar, 3 μm.

cent nuclei, with prominent nucleoli, showing arborization of the cytoplasm toward the IPL (Figs. 24, 25). In the middle region of the INL, nuclei with characteristics similar to the amacrine nuclei were observed that probably correspond to bipolar cells (Fig. 24). Processes of bipolar cells could be seen penetrating the IPL and exhibiting diverse types of synapses, some of them with ribbonlike, dense structures (Figs. 25, 25a). These bipolar processes also received input, the so-called reciprocal synapses, from amacrine cells (Fig. 25a). Some axosomatic synapses were seen on amacrine cells (Fig. 26). In the IPL, which was rather well developed, other types of synapses were observed. Of the two main types of synaptic vesicles distinguished, most had electrolucent contents, but a minority displayed electrodense contents (Fig. 26).

In the GCL, two main types of cells were observed (Fig. 27). Type I ganglion cells displayed rounded nuclei of large size, approximately 8 μm in diameter, and reduced heterochromatic component. The nucleus of type II cells, approximately 5 μm in diameter, presented invaginations of the nuclear envelope and more heterochromatin than that of type I. Nucleoli were prominent in both types. In the type II cells, the nucleus and the entire soma were smaller than in type I cells. Many rER cisterns, a well-developed Golgi apparatus, and numerous mitochondria were observed in type I cells (Fig. 28). Some synapses were detected in the ganglion cell somata (Figs. 29, 29a). Occasionally, ganglion cells did not form a single stratified row, but appeared to be organized in a column invading the IPL (Fig. 30).

DISCUSSION

The mole rat *S. ehrenbergi* represents a beautiful model for the study of mosaic evolutionary remodeling, in this case triggered by adaptation to a nearly complete subterranean lifestyle.[24] This has resulted in a complete loss of visual function and large-scale regression of corresponding brain structures,[7] as well as in ocular regression with degeneration of the lens.[25]

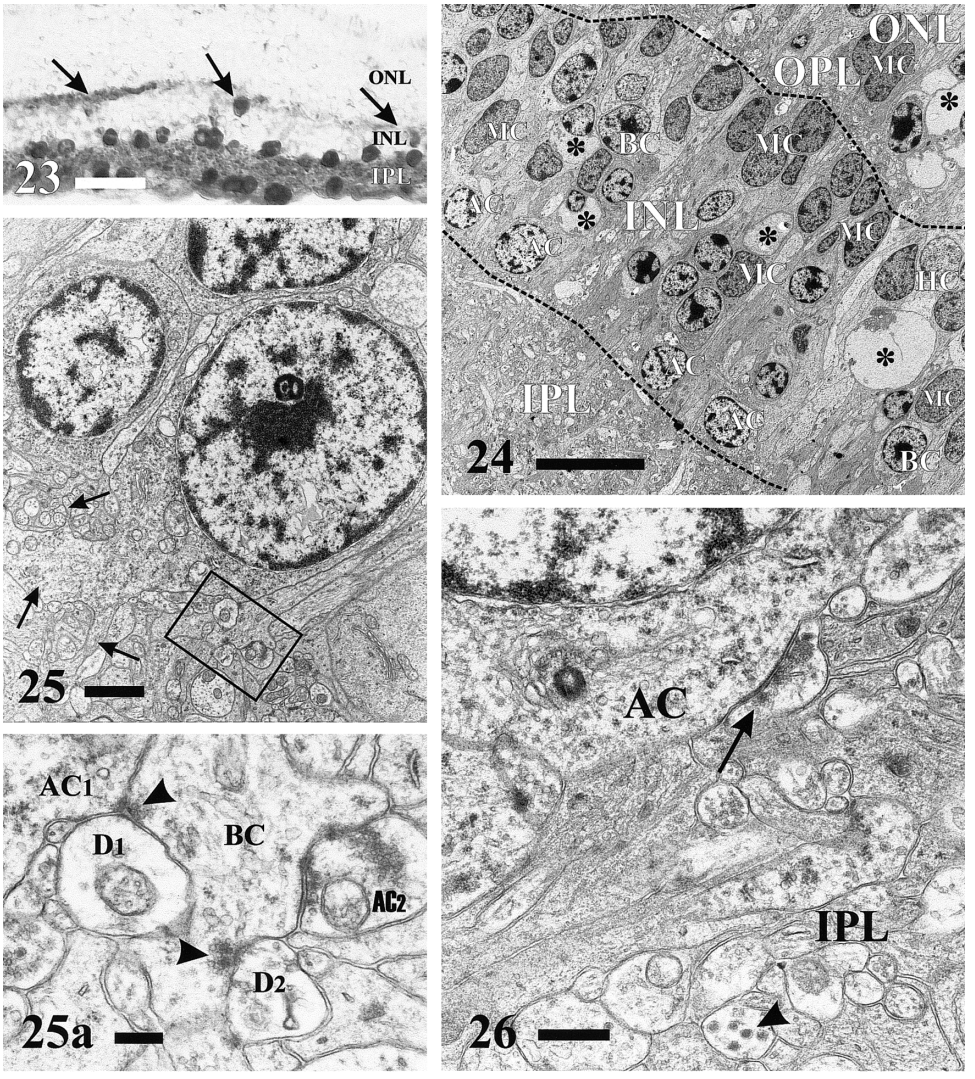

Figure 23. Anti-calretinin labeling was found at both the inner and outer edges of the INL, in the amacrine cell and horizontal cell (*arrows*) sublayers, and in some cell somata of the GCL. Middle-sectioned somata showed strong cytosolic staining with clear nuclei, in agreement with many observations that calretinin has a cytosolic location. Occasional apparent staining in the nucleus of some somata, which were cut more tangentially, most likely is a two-dimensional image delusion, due to intense cytosolic staining that masked the nucleus. The IPL was completely labeled but did not show the bands characteristic in sighted mammals. Bar, 25 μm.

Figure 24. At the EM level, the INL (with oblique position and delimited by discontinuous lines in this micrograph) showed diverse cell types. Müller cells (MC) were abundant and sometimes were displaced toward the ONL (*right upper corner*). A likely horizontal cell (HC) and some likely bipolar cells (BC) were also noted. (✻) Displaced PCs. Amacrine cells (AC) formed a well-defined population in the lower margin of the INL. Bar, 10 μm.

Figure 25. An amacrine cell typically displayed a large, round nucleus with prominent nucleolus and cytoplasmic processes toward the IPL (*black arrows*). *Box*: a bipolar cell process, which is magnified in Figure 25a. Bar, 1 μm.

Figure 25a. This bipolar cell (BC) axonal process showed two synapses (*arrowheads*): one on the amacrine cell described in the Figure 25 (AC1) and on an unidentified dendritic process (D1) and the second, showing two ribbons, on another unidentified dendritic process (D2). D1 and D2 could belong either to amacrine or ganglion cells. This bipolar axon also received input from another amacrine cell process (AC2). Bar, 0.25 μm.

Figure 26. An amacrine cell (AC) received a synapse on its soma (*arrow*). In the IPL, many of the vesicles seen in the axonal processes were small and showed electrolucent content, but some of them had electrodense content (*arrowhead*). Bar, 0.5 μm.

However, the retina retains its morphologic integrity to a surprisingly large extent, with the persistence of rather well organized layers. Although there is a distinct change in photoreceptor morphology, the mole rat retina profoundly differs from animal models of retinal degeneration, in that a total absence of visual function does not imply a total loss of visual photoreceptor cells or of second-order neurons. We present in this study a comprehensive morphologic analysis of the *Spalax*

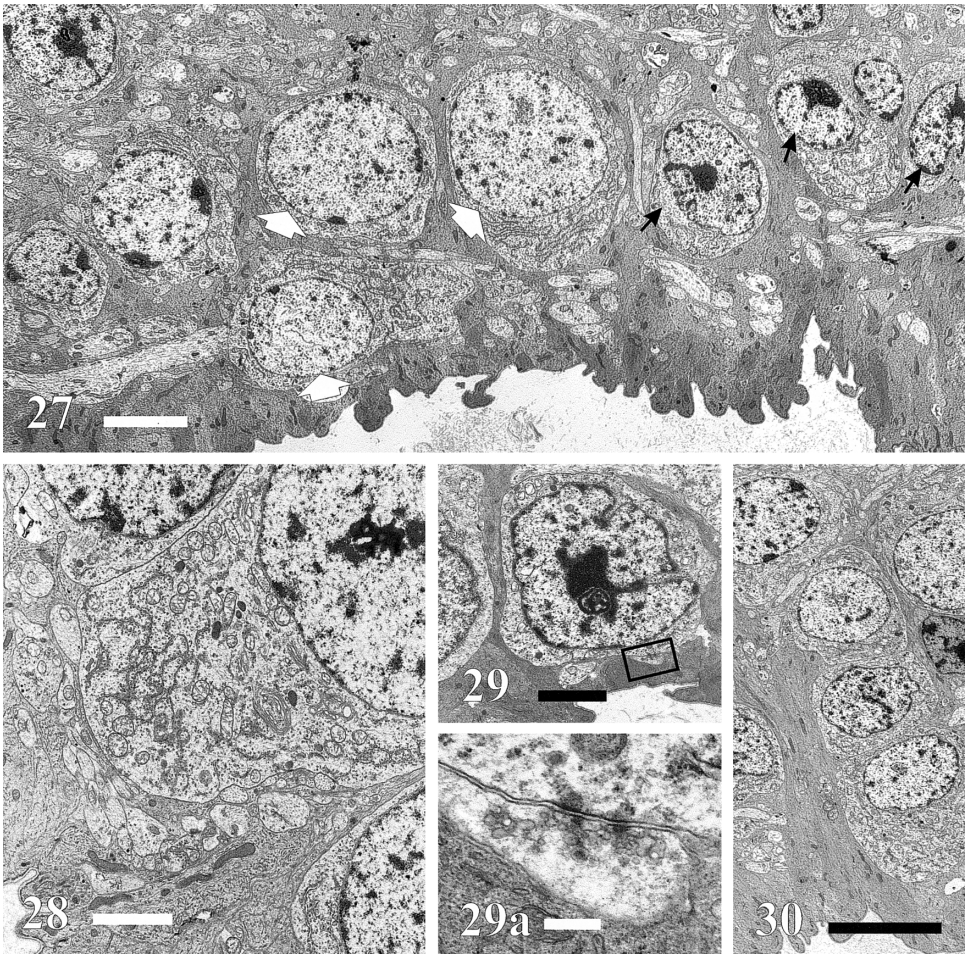

FIGURE 27. At least two ganglion cell types were distinguished. Type I cells (*white arrows*) had a large, round nucleus with little heterochromatin, and type II cells (*black arrows*) showed a smaller, more heterochromatic nucleus and invaginations of the nuclear envelope. Bar, 5 μm.

FIGURE 28. Type I ganglion cells possessed many different organellae in their cytoplasm, indicating high cellular activity. Bar, 2 μm.

FIGURE 29. The cytoplasm of type II ganglion cells had less indicators for biosynthetic activity. *Box*: the synapse magnified in Figure 29a. Bar, 2 μm.

FIGURE 29A. Axosomatic synapse on a type II ganglion cell. Vesicles with electrolucent as well as electrodense contents were observed in the synaptic ending. Bar, 0.25 μm.

FIGURE 30. Occasionally ganglion cells were not located in a single row, but were displaced and extend column-wise into the overlying IPL. Bar, 10 μm.

retina and provide strong support for the hypothesis that this organ has been reorganized to mediate entirely the photoperiodic biology of the mole rat. In the following sections we will discuss these various aspects in more detail.

The retina of the mole rat showed a quite normal organization. All the layers and cell types of the mammalian retina were detectable, with the exception of cone cells, whose presence, despite some circumstantial evidence, could not yet be directly demonstrated.

The observed morphology of the PCs did not correspond to the classic rod or cone cells, because the OS did not display the normal stacked organization, but were rudimentary and composed of whorls of membranes. These are quite similar to those reported in the mole retina[26] and, particularly remarkable, in the OS of the avian pinealocytes.[27–29] Although in most avian species, pinealocytes are not connected to second-order neurons, some exceptions occur, such as passerine birds, in which these neurons are abundant.[27]

In sighted rodents, such as the mouse, rod and cone nuclei show some differential ultrastructural features, which allow them to be distinguished.[30] In *Spalax,* the nuclei observed in the ONL all had a similar appearance and the rod-opsin immunolabeling indicated that in our samples the majority, if not all, of the cells in this layer were rods. In fact, we did not detect immunolabeling in *Spalax* with CERN-906, an antibody that is a good marker for the green cone cells in other rodents, such as mouse.[31] Our antibodies have been shown before to be monospecific for these *Spalax* phototransduction-related proteins as well.[14,32] This does not necessarily imply, of course, that cone cells are entirely absent in the mole rat retina. In fact, David-Gray et al.[13,32] have provided evidence that the mole rat retina expresses a green-cone–like opsin, which is one of the most "red-shifted" photopigments found in rodents. However, the location of this opsin has not been established yet, and it need not originate in cone cells.

The PC pedicles in the mole rat retina did not exhibit the degree of organization reported in most sighted mammals. The presence of ribbon fields, sometimes in regions distant from the synaptic site, the so called "active zone",[33] suggests a storage of part of the synaptic machinery. Similar synaptic ribbon plasticity has also been observed in the retina of hibernating squirrels,[34] and, in fact, in the pineal of most mammals, as well.[35] The mammalian rod cell normally uses a single active zone at its pedicle.[36] It might thus be suspected that some photoreceptor endings in the mole rat retina exhibiting multiple synaptic sites correspond to cone cells. Actually, images of other mammalian cone terminals reported in the literature[37] show a much more complex organization. Some investigators[38,39] have reported that cone pedicles have approximately 20 active zones, many more than the examples observed in our samples. However, the presence of calretinin-positive horizontal cells in the *Spalax* retina (see later discussion) may also reflect the presence of cone-cells, because the three types of horizontal cells described in sighted mammals all interconnect cone pedicles, either with other cone cells or with rod cell spherules.[40] Hence, the question of whether cone cells persist in *Spalax* is still open and requires more specific cone-directed assays.

Even though that some displaced cells were found, the *Spalax* retina displayed a stratified organization similar to that reported for sighted vertebrates. Although calretinin-positive horizontal cells have also been found in other species, including a rodent such as the rat,[41] the calretinin-positive distribution found in *Spalax* strongly resembles the one identified in the mouse with anti-calbindin antibodies.[20]

The lamination of the IPL reported in other mammals[20] was absent in *Spalax*, and this indicates that the inner layers of its retina have a lower degree of organization than that observed in sighted animals. Nevertheless, as indicated by morphology and the immunolabeling at the LM and the EM levels, amacrine, bipolar, and ganglion cells were well represented, and synaptic contacts among them were well established. Calretinin-immunopositive amacrine cells, which are the so called "AII" or "rod amacrine cells" in other mammals,[42,43] seemed to represent most of the amacrine population in *Spalax*. The pattern of synaptic contacts in the IPL was diverse and not easy to interpret in ultrastructural images without the use of any type of labeling, which is outside the context of the present study. It is widely accepted, however, that ribbonlike densifications in the IPL belong exclusively to bipolar cells. To distinguish cone and rod bipolar cells by their ultrastructure or the position of their terminals in the IPL is problematic, because these aspects may vary, depending on the species. Taking this into account, the images we present could correspond to cone as well as rod bipolar cells. To differentiate at the EM level between AII amacrine cells and other types at the EM level is not easy, either. In other mammals, AII cells receive input from rod bipolar cells, but they usually make chemical output synapses with cone bipolar cells and ganglion cells. Considering that the population of cone bipolar cells, if present, would be a small minority, we present the most likely explanation, in our opinion, for the synaptic contacts observed between bipolar and amacrine cells in Figures 25 and 26.

The cell type showing organellae-free cytoplasmic areas described in our results undoubtedly had the characteristics of the rod cells described in the ONL, with the exception that no OS was present. It is not clear presently why they occupy such a displaced position in the retina. Rod opsin IR and also the presence of established synapses suggest that these cells may have retained some kind of photoreceptor function.

Taking into account all these considerations, we conclude that the retina of *Spalax* presents the morphology of a functional organ, with no evidence of a severe differentiation-related degenerative process. In addition, in view of the absence of apoptotic cells in our samples, which were taken from adult individuals, there is no evidence for a slow aging-connected degenerative process, as is demonstrated, for instance, in the *rds* mouse, which also displays rudimentary OS.[44]

Strong evidence for a photosensory function of the *Spalax* retina was provided by the presence of intact synaptic organization throughout the retinal layers. This was further supported by the abundant presence of PC pedicles and strong rod-opsin and transducin immunolabeling. In addition, as Janssen et al.[14] have demonstrated, the *Spalax* rod visual pigment is fully functional, and light stimulation triggers c-fos expression in the SCN.[9] Also, rod-opsin–positive phagosomes are detectable in the RPE, demonstrating that the OS undergo their typical turnover process.

Although the strongest rod-opsin labeling was observed in the rudimentary OS, the entire cell membrane exhibited a positive reaction. This could indicate that the entire PC has become photoactive, complying with the loss of pressure to maintain proper image-detection. In fact, most of the light reaching the eye of the mole rat probably enters laterally through an unpigmented area of the hairy skin[12] and not frontally, because of the strong filtering effect of the pigmentary cap. In addition, the folds observed in the *Spalax* retina, quite similar to those found in the avian pineal[29] and in the retina of megachiroptean bats,[45] would no longer interfere with image resolution. We confirm the LM observation of Janssen et al.[14] that α-transducin IR is restricted to the rudimentary OS at the TEM level. This may restrict a photosensory function to the OS, but we cannot exclude that the putatively lower levels of transducin near the plasma membrane may yet have escaped immunodetection. The release of the severe spatial constraints, imposed on rhodopsin in the highly organized disc membranes of the OS in sighted animals, may also explain why *Spalax* rhodopsin complies with much larger carbohydrate antennae.[14]

All the mentioned morphologic features indicate that the *Spalax* retina has adopted features of the pineal of nonmammalian vertebrates and hence suggest strongly, in line with earlier suggestions,[12–14,30] that it has evolved toward a nonvisual photosensory function**.** The arguments for this affirmation presented in this manuscript can be summarized as follows.

The subcutaneous location of the *Spalax* eye and its diffuse light input are similar to the situation faced by the avian pinealocytes. The abnormal OS organization, a likely evolutionary acquisition, is also similar to avian pinealocytes, wherein the function in photoperiodic physiology does not require neatly stacked visual pigment. The synaptic ribbon fields and their plasticity have also been reported in the pinealocytes of mammalian and nonmammalian vertebrates.[35] Finally, the retinal folds observed in our samples resemble those found in the avian pineal gland[29] and in the retina of some nocturnal mammals.[45] In fact, the histologic structure of the pineal organ of some higher vertebrates, such as avians, has been described as a "folded retina."[46]

Conclusions

Although the mole rat constitutes an example of severe ocular regression, it profoundly differs from animal models for retinal degeneration described in sighted mammals. The ultrastructure and immunolabeling pattern of the photoreceptor cells support our previous hypothesis that they represent functional receptors. Our observations further indicate that neither loss of connectivity or of secondary neurons, nor loss of a particular type of cell or synapse occurs in the inner layers of the mole rat retina. With a visual task excluded, all evidence leads to the

conclusion that this unique organ has been preserved and reorganized to mediate light-dependent entrainment of circadian and circannual rhythms.

Acknowledgments

The authors are grateful to David Hicks, from the National Institute of Health and Medical Research (Strasburg, France), for providing the rho 4D2 antiserum.

References

1. Foster RG, Provencio I, Hudson D, Fiske S, De Grip WJ, Menaker M. Circadian photoreception in the retinally degenerate mouse (*rd/rd*). *J Comp Physiol* [*A*]. 1991;169:39–50.
2. Provencio I, Wong S, Lederman AB, Argamaso SM, Foster RG. Visual and circadian responses to light in aged retinally degenerate mice. *Vision Res.* 1994;34:1799–1806.
3. Freedman MS, Lucas RJ, Soni B, et al. Regulation of mammalian circadian behavior by non-rod, non-cone, ocular photoreceptors. *Science.* 1999;284:421–422.
4. Lucas RJ, Freedman MS, Muñoz M, García-Fernández JM, Foster RG. Regulation of the mammalian pineal by non-rod, non-cone, ocular photoreceptors. *Science.* 1999;284:505–507.
5. Czeisler CA, Shanahan TL, Klerman EB, et al. Suppression of melatonin secretion in some blind patients by exposure to bright light. *N Engl J Med.* 1995;332:6–11.
6. Sanyal S, Jansen HG, De Grip WJ, Nevo E, De Jong WW. The eye of the blind mole rat, *Spalax ehrenbergi*: rudiment with hidden function? *Invest Ophthalmol Vis Sci.* 1990;31:1398–1404.
7. Cooper HM, Herbin M, Nevo E. Visual system of a naturally microphthalmic mammal: the blind mole rat, *Spalax ehrenbergi. J Comp Neurol.* 1993;328:313–350.
8. Bronchti G, Rado R, Terkel J, Wollberg Z. Retinal projections in the blind mole rat: a WGA-HRP tracing study of a natural degeneration. *Brain Res Dev Brain Res.* 1991;58:159–170.
9. Vuillez P, Herbin M, Cooper HM, Nevo E, Pévet P. Photic induction of Fos immunoreactivity in the suprachiasmatic nuclei of the blind mole rat (*Spalax ehrenbergi*). *Brain Res.* 1994;654:81–84.
10. Pévet P, Heth G, Hiam A, Nevo E. Photoperiod perception in the blind mole rat (*Spalax ehrenbergi*, Nehring): involvement of the Harderian gland, atrophied eyes, and melatonin. *J Exp Zool.* 1984;232:41–50.
11. Avivi A, Albrecht U, Oster H, Joel A, Beiles A, Nevo E. Biological clock in total darkness: the *Clock/MOP3* circadian system of the blind subterranean mole rat. *Proc Natl Acad Sci USA.* 2001;98:13751–13756.
12. Cooper HM, Herbin M, Nevo E. Ocular regression conceals adaptative progression of the visual system in a blind subterranean mammal. *Nature.* 1993;361:156–159.
13. David-Gray ZK, Cooper HM, Janssen JWH, Nevo E, Foster RG. Spectral tuning of a circadian photopigment in a subterranean "blind" mammal (*Spalax ehrenbergi*). *FEBS Lett.* 1999;461:343–347.
14. Janssen JWH, Bovee-Geurts PHM, Peeters ZPA, et al. A fully functional rod visual pigment in a blind mammal: a case for adaptative functional reorganization? *J Biol Chem.* 2000;275:38674–38679.
15. Nevo E, Ivanitskaya E, Beiles A. *Adaptative radiation of blind subterranean mole rats. Naming and revisiting the four sibling species of the* Spalax ehrenbergi *superspecies in Israel:* Spalax galili *(2n=52),* S. golani *(2n=54),* S. carmeli *(2n=58) and* S. judaei *(2n=60).* Leiden, The Netherlands: Backhuys; 2001.
16. Hicks D, Molday RS. Differential immunogold-dextran labelling of bovine and frog rod and cone cells using monoclonal antibodies again bovine rhodopsine. *Exp Eye Res.* 1986;42:55–71.
17. Schalken JJ, De Grip WJ. Enzyme-linked immunosorbent assay for the quantitative determination of the visual pigment rhodopsin in total eye extracts. *Exp Eye Res.* 1986;43:431–439.
18. Janssen JJM. The rod visual pigment rhodopsin: in vitro expression and site specific mutagenesis. PhD thesis. University Of Nijmegen, The Netherlands; 1991.
19. Foster RG, García-Fernández JM, Provencio I, De Grip WJ. Opsin localization and chromophore retinoids identified within the basal brain of the lizard. *Anolis carolinensis. J Comp Physiol* [*A*]. 1993;172:33–45.
20. Haverkamp S, Wässle H. Immunocytochemical analysis of the mouse retina. *J Comp Neurol.* 2000;424:1–23.
21. Sternberger L A. *Immunocytochemistry.* 2nd ed. New York: John Wiley & Sons; 1979.
22. Negoescu A, Lorimier P, Labat-Moleur F, et al. In situ apoptotic cell labeling by the TUNEL method: improvement and evaluation on cell preparations. *J Histochem Cytochem.* 1996;44:959–968.
23. Hacker G. The morphology of apoptosis. *Cell Tissue Res.* 2000;301:5–17.
24. Nevo E. *Mosaic Evolution of Subterranean Mammals: Regression, Progression, and Global Convergence.* Oxford, UK: Oxford University Press; 1999.
25. Avivi A, Joel A, Nevo E. The lens protein α-B-crystallin of the blind subterranean mole-rat: high homology with sighted mammals. *Gene.* 2001;264:45–49.
26. Grim JN. Whorl-like outer segments in the retina of the mole (*Scalopus aquaticus*). *Acta Anat* (*Basel*). 1990;138:261–264.
27. Oksche A, Kirschstein H. Electron microscopic studies of the pineal organ in *Passer domesticus. Z Zellforsch Mikrosk Anat.* 1969;102:214–241.
28. Oksche A, Kirschstein H, Kobayashi H, Farner DS. Electron microscopic and experimental studies of the pineal organ in the white-crowned sparrow, *Zonotrichia leucophrys gambelii. Z Zellforsch Mikrosk Anat.* 1972;124:247–274.
29. Fejér Z, Röhlich P, Szél A, et al. Comparative ultrastructure and cytochemistry of the avian pineal organ. *Microsc Res Tech.* 2001;53:12–24.
30. Carter-Dawson LD, LaVail MM. Rods and cones in the mouse retina. I: structural analysis using light and electron microscopy. *J Comp Neurol.* 1979;188:245–262.
31. Jiménez AJ, García-Fernández JM, González B, Foster RG. The spatio-temporal pattern of photoreceptor degeneration in the aged *rd/rd* mouse retina. *Cell Tissue Res.* 1996;284:193–202.
32. David-Gray ZK, Janssen JW, De Grip WJ, Nevo E, Foster RG. Light detection in a 'blind mammal'. *Nat Neurosci.* 1998;1:655–656.
33. Gray EG, Pease HL. On understanding the organisation of the retinal receptor synapses. *Brain Res.* 1971;35:1–15.
34. Vollrath L, Spiwoks-Becker I. Plasticity of retinal ribbon synapses. *Microsc Res Tech.* 1996;35:472–487.
35. Vollrath L. The pineal organ. In: Vollrath L, Oksche A, eds. *Handbuch der mikroskopichen Anatomie des Menschen*. Vol. 6. Berlin: Springer Verlag; 1981:147–158.
36. Ahnelt PK, Keri C, Kolb H. Identification of pedicles of putative blue sensitive cones in human and primate retina. *J Comp Neurol.* 1990;293:39–53.
37. Haverkamp S, Grunert U, Wässle H. The cone pedicle, a complex synapse in the retina. *Neuron.* 2000;27:85–95.
38. Ahnelt PK, Kolb H. Horizontal cells and cone photoreceptors in primate retina: a Golgi-light microscope study of spectral connectivity. *J Comp Neurol.* 1994;343:387–405.
39. Kolb H, Goede P, Roberts S, McDermott, Gouras P. Uniqueness of the S-cone pedicle in the human retina and consequences for color processing. *J Comp Neurol.* 1997;386:443–460.
40. Kolb H. The connexions between horizontal cells and photoreceptors in the retina of the cat: electron microscopy of Golgi-preparations. *J Comp Neurol.* 1974;155:1–14.
41. Pasteels B, Rogers J, Blachier F, Pochet R. Calbindin and calretinin localization in retina from different species. *Vis Neurosci.* 1990;5:1–16.
42. Massey SC, Mills SL. Antibody to calretinin stains AII amacrine cells in the rabbit retina: double-label and confocal analyses. *J Comp Neurol.* 1999;411:13–18.
43. Wässle H, Grunert U, Chun MH, Boycott BB. The rod pathway of the macaque monkey retina: identification of AII-amacrine cells with antibodies against calretinin. *J Comp Neurol.* 1995;361:537–551.
44. Jansen HG, Sanyal S, De Grip WJ, Schalken JJ. Development and degeneration of retina in rds mutant mice: ultraimmunohistochemical localization of opsin. *Exp Eye Res.* 1987;44:347–361.
45. Fejér Z, Haldar C, Ghosh M, et al. Pineal organ-like organization of the retina in megachiroptean bats. *Acta Biol Hung.* 2001;52:17–27.
46. Vígh B, Rohlich P, Gorcs T, et al. The pineal organ as a folded retina: immunohistochemical localization of opsins. *Biol Cell.* 1998;90:653–659.